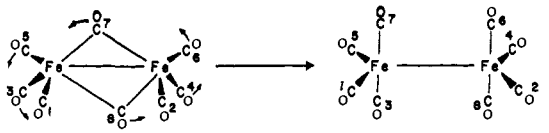

Figure 2. A diagram showing how the CO ligands associated with the bridged edge of the Fe_3 triangle would shift as the bridges are opened in a concerted manner.

the molecule. This can be appreciated easily with the aid of Figure 2, which shows only one edge of the Fe_3 triangle and omits, for clarity, the other $Fe(CO)_4$ group which actually lies below the plane of the paper. We begin with a bridged structure on this edge and move the bridging CO groups out of bridging positions in a counterclockwise sense, as indicated by the arrows. This leads to a $Ru_3(CO)_{12}$ type structure, in which the carbonyls numbered 3, 6, 7, and 8 are axial and 1, 2, 4, and 5 are equatorial. However, if the bridges had been rotated out in the opposite sense, the axial groups would have been 4, 5, 7, and 8 and the equatorial ones 1, 2, 3, and 6. If these processes are now repeated successively on the other two edges of the Fe_3 triangle, *all* CO groups will be scrambled (1) over the metal atoms, (2) over both axial and equatorial positions of the $Ru_3(CO)_{12}$ structure, and (3) over both of the bridging and all of the terminal positions of the bridged structure.

Acknowledgment. We are very grateful to The Robert A. Welch Foundation for direct support of this work through Research Grant A494 and for funds used to purchase the diffractometer and to the National Science Foundation for support under Grant No. 33142X. We thank Dr. B. A. Frenz for helpful discussions.

Supplementary Material Available. Tables of observed and calculated structure factor amplitudes and root-mean-square amplitudes of thermal vibration will appear following these pages in the microfilm edition of this volume of the journal. Photocopies of the supplementary material from this paper only or microfiche (105 × 148 mm, 24× reduction, negatives) containing all of the supplementary material for the papers in this issue may be obtained from the Journals Department, American Chemical Society, 1155 16th St. N.W., Washington, D. C. 20036. Remit check or money order for $3.00 for photocopy or $2.00 for microfiche, referring to code number JACS-74-4155.

Synthetic Analogs of the Active Sites of Iron–Sulfur Proteins. VI.[1] Spectral and Redox Characteristics of the Tetranuclear Clusters $[Fe_4S_4(SR)_4]^{2-}$

B. V. DePamphilis, B. A. Averill,[2] T. Herskovitz, L. Que, Jr., and R. H. Holm*

Contribution from the Department of Chemistry, Massachusetts Institute of Technology, Cambridge, Massachusetts 02139. *Received January 30, 1974*

Abstract: The electronic spectra (250–700 nm) and redox properties of a series of tetrameric complexes $[Fe_4S_4(SR)_4]^{2-}$ (R = alkyl, aryl, Ac-Cys-NHMe) have been examined in nonaqueous and aqueous DMSO solutions. $[Fe_4S_4(S\text{-}Cys(Ac)NHMe)_4]^{2-}$ and $[Fe_4S_4(SC_6H_4NMe_3)_4]^{2+}$ were generated in solution by ligand substitution reactions of the free thiols and $[Fe_4S_4(S\text{-}t\text{-}Bu)_4]^{2-}$. Alkyl-substituted tetramers possess two principal absorption bands whose positions (297–308, 417–421 nm) and intensities reveal a relationship with the two prominent absorptions in the spectra of the reduced "high-potential" (HP_{red}) and oxidized ferredoxin (Fd_{ox}) proteins. Aryl-substituted tetramers have maxima at 455–510 nm. Polarographic results reveal the electron transfer series $[Fe_4S_4(SR)_4]^z$ with $z = 4-, 3-, 2-$, and $1-$; the $2-/3-$ process is reversible or nearly reversible in all cases. Half-wave potentials for this process involving tetramers with R = alkyl and $p\text{-}C_6H_4X$ [X = H, Me, $^+NMe_3$ ($2+/1+$ couple)] are linearly correlated with the σ^* and σ_p substituent constants, respectively. The relationship between the total oxidation levels, z, of the synthetic analogs and those of the proteins is summarized. Spectra and $2-/3-$ potentials of $[Fe_4S_4(S\text{-}Cys(Ac)NHMe)_4]^{2-}$ in DMF, DMSO, and DMSO–H_2O are somewhat solvent dependent, and most closely resemble the corresponding properties of HP_{red} and Fd_{ox} in aqueous DMSO or water solution. Half-wave potentials in DMSO–H_2O after correction for apparent liquid junction potentials are near the values estimated for reduction of HP_{red} to $HP_{s\text{-}red}$ in this solvent but are estimated to be *ca.* 0.2–0.6 V more negative than E_0' values for Fd_{ox}/Fd_{red} in aqueous solution. These and other results indicate that the protein structure and environment make a significant contribution to the redox potentials of the iron–sulfur clusters.

Ferredoxins and other iron–sulfur proteins[3,4] form a comprehensive class of nonheme iron proteins which are implicated as electron carriers in diverse processes of cell metabolism.[5] The electron-carrying properties of these proteins are related to the ability of their iron–sulfur active sites to exist in several different oxidation levels interrelated by one-electron transfer reactions. In order to provide further clarification of the nature of these active sites, we are engaged in a program directed toward the synthesis and structural and electronic characterization of low molecular weight iron–sulfur complexes which serve as close representa-

(1) Part V: R. H. Holm, W. D. Phillips, B. A. Averill, J. J. Mayerle, and T. Herskovitz, *J. Amer. Chem. Soc.*, **96**, 2109 (1974).

(2) National Science Foundation Predoctoral Fellow, 1969–1972.

(3) (a) J. C. M. Tsibris and R. W. Woody, *Coord. Chem. Rev.*, **5**, 417 (1970); (b) D. O. Hall, R. Cammack, and K. K. Rao, *Pure Appl. Chem.*, 34, 553 (1973); (c) W. H. Orme-Johnson, *Annu. Rev. Biochem.*, 42, 159 (1973).

(4) G. Palmer and H. Brintzinger in "Electron and Coupled Energy Transfer in Biological Systems," Vol. 1, Part B, T. E. King and M. Klingenberg, Ed., Marcel Dekker, New York, N. Y., 1972, Chapter 9.

(5) B. B. Buchanan and D. I. Arnon, *Advan. Enzymol. Relat. Subj. Biochem.*, 33, 119 (1970).

tions of such sites. Recently, we have reported the synthesis and characterization of $[FeS(SCH_2)_2C_6H_4]_2^{2-}$[6] and $[Fe_4S_4(SR)_4]^{2-}$,[1,7-10] which serve as analogs of the active sites of 2-Fe plant, bacterial, and mammalian and 4- and 8-Fe bacterial proteins, respectively. The D_{2d} structure, **1**, has been established for the R = CH_2Ph[7,8]

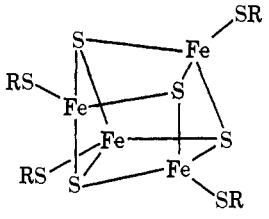

1

and Ph[9b] members of an extensive series of tetranuclear dianions with R = alkyl or aryl.[1,8,9] The resemblance of these species to the iron–sulfur clusters in the proteins is borne out by several lines of evidence. At the reported stages of refinement of the protein structures, the cluster stereochemistry of **1** is nearly congruent with the active site structures of the oxidized 8-Fe ferredoxin (Fd_{ox}) from *Peptococcus aerogenes*[11,12] and the reduced 4-Fe "high-potential" protein (HP_{red}) from *Chromatium*.[12] Comparison of various electronic properties of $[Fe_4S_4(SCH_2Ph)_4]^{2-}$ with those of the proteins has shown that the dianion, Fd_{ox}, and HP_{red} possess the same total oxidation level.[7] In addition, the electronic properties of $[Fe_4S_4(SR)_4]^{3-}$,[13] which include "g = 1.94 type" epr spectra, are closely related to those of Fd_{red} proteins.

The results summarized above and others described elsewhere[1,6-8,13] reveal that close representations of the Fe–S cluster, which constitutes the active centers of 4-Fe and 8-Fe proteins, can be formed in the absence of the cysteinyl-containing polypeptides found in these proteins. Comparison of properties of the proteins and the synthetic analogs in the same total oxidation level affords the previously unavailable opportunity to explore the influence of protein structure and environment on these properties. The most significant biophysical function of the 4-Fe and 8-Fe ferredoxins appears to be their ability to transfer electrons at potentials near that of the hydrogen electrode. Potentials for the majority of these proteins occur at E_0' values in the vicinity of −0.40 V. As noted earlier[7] these potentials are decidedly less negative than that for $[Fe_4S_4(SCH_2Ph)_4]^{2-/3-}$ when compared on the same scale. In order to provide a fuller definition of the redox potentials and electronic transfer capacity of the tetranuclear clusters, the electrochemical behavior of a variety of the complexes, **1**, with R = alkyl or aryl have been investigated by polarographic methods in nonaqueous and partially aqueous media. In addition, ultraviolet and visible spectra of a series of $[Fe_4S_4(SR)_4]^{2-}$ complexes in these media are reported in order to provide further evidence of the electronic similarity between the dianionic analogs and HP_{red} and Fd_{ox}.

Experimental Section

Preparation of Compounds. ***N*-Acetyl-*S*-benzyl-L-cysteine (Ac-L-Cys(Bzl)OH).** This compound was prepared from *S*-benzyl-L-cysteine[14] (mp 228–232° dec; $[\alpha]^{20}D$ +29.7 (*c* 1.0, 1.0 *N* NaOH)) and acetic anhydride using the method of Cash.[15] After treatment with charcoal in hot ethanol and filtration, the solvent was removed, and the crude product was recrystallized from isopropyl alcohol–hexane to give Ac-L-Cys(Bzl)OH in 88% yield: mp 145.5–147°, $[\alpha]^{20}D$ −49.0 (*c* 1.0, 95% ethanol) [lit. mp 143.5–145.5°, $[\alpha]^{22}D$ −46.1 (*c* 1, 95% ethanol);[15] mp 143–144°, $[\alpha]^{26}D$ −41.5 (*c* 1, 95% ethanol)[16]].

3-*O*-(*N*-Acetyl-*S*-benzyl-L-cysteinyl)-2,3-dihydroxy-*N*-ethylbenzamide (Ac-L-Cys(Bzl)NEV). A solution of 25.3 g (0.10 mol) of Ac-Cys(Bzl)OH in 100 ml of 1 *N* NaOH, 100 ml of water, and 20 ml of pyridine was taken to pH 4.5 with 3 *N* HCl. Ethyl acetate (250 ml) was added, the reaction mixture was cooled in ice to 10°, and, while stirring vigorously, 27.6 g of 2-ethyl-7-hydroxybenzisoxazolium tetrafluoroborate[17] (NEVBF, 0.11 mol) was added as a solid in small portions over 40 min. The mixture was stirred for a further 30 min while warming to room temperature, at which point the precipitated product was collected by filtration and pressed dry. The filtrate was separated, and the aqueous phase was extracted with ethyl acetate (2 × 50 ml). The combined organic phases were washed with 3 *N* HCl (200 ml), water (200 ml), 0.5 *N* $NaHCO_3$ (400 ml), and saturated aqueous NaCl (200 ml) plus 3 *N* HCl (50 ml). The organic phase was combined with the solid obtained by filtration, more warm ethyl acetate was added to dissolve the solid entirely, and the solution was dried over $MgSO_4$. After filtration the solution was reduced in volume and isooctane was added to incipient crystallization. Slow cooling to −20° afforded 37 g (89%) of the active ester Ac-L-Cys(Bzl)NEV: mp 112–117°, $[\alpha]^{20}D$ −54.5 (*c* 2.5, DMF). The pmr spectrum was consistent with the indicated formulation. *Anal.* Calcd for $C_{21}H_{24}N_2SO_5$: C, 60.56; H, 5.81; N, 6.73; S, 7.70. Found: C, 60.54; H, 5.66; N, 6.59; S, 7.83.

***N*-Acetyl-*S*-benzyl-L-cysteine-*N*-methylamide (Ac-L-Cys(Bzl)-NHMe).** Methylamine was bubbled through a solution of 0.57 g (5 mmol) of 1,1,3,3-tetramethylguanidine in 5 ml of DMSO for 30 min. Ac-Cys(Bzl)NEV (2.08 g, 5.0 mmol) was added as a solid over 45 min to the rapidly stirred solution while maintaining a flow of methylamine. The mixture was stirred for an additional 60 min under a methylamine atmosphere and was then distributed between 50 ml of ethyl acetate and 50 ml of 3 *N* HCl. The layers were separated, and the pink aqueous phase was extracted with ethyl acetate (2 × 25 ml). The combined organic phases were washed with water (50 ml), 0.5 *N* $NaHCO_3$ (100 ml), and saturated aqueous NaCl (50 ml) plus 3 *N* HCl (10 ml), dried over $MgSO_4$, and evaporated. The residue was recrystallized from ethyl acetate–isooctane to give 0.74 g (55%) of AcCys(Bzl)NHMe: mp 153.5–156.0°, $[\alpha]^{20}D$ −33.8 (*c* 2.4, DMF). The pmr spectrum was consistent with the indicated formulation. *Anal.* Calcd for $C_{13}H_{18}N_2O_2S$: C, 58.62; H, 6.81; N, 10.52; S, 12.04. Found: C, 58.69; H, 6.73; N, 10.41; S, 11.96.

***N*-Acetyl-L-cysteine-*N*-methylamide (Ac-L-Cys-NHMe).** Approximately 500 ml of liquid NH_3 was distilled from metallic sodium into a 1-l. three-necked flask equipped a magnetic stirring bar and a Dry Ice condenser and containing 19.5 g (73.3 mmol) of Ac-Cys(Bzl)NHMe. To the vigorously stirred refluxing solution was added 3.37 g (147 mmol) of metallic sodium in 40–50 mg pieces. When a permanent blue color appeared, NH_4Cl (16 g, 150 mmol) was added immediately to discharge the color. The solvent was evaporated under a stream of nitrogen, and the flask was evacuated

(6) J. J. Mayerle, R. B. Frankel, R. H. Holm, J. A. Ibers, W. D. Phillips, and J. F. Weiher, *Proc. Nat. Acad. Sci. U. S.*, **70**, 2429 (1973).
(7) T. Herskovitz, B. A. Averill, R. H. Holm, J. A. Ibers, W. D. Phillips, and J. F. Weiher, *Proc. Nat. Acad. Sci. U. S.*, **69**, 2437 (1972).
(8) B. A. Averill, T. Herskovitz, R. H. Holm, and J. A. Ibers, *J. Amer. Chem. Soc.*, **95**, 3523 (1973).
(9) (a) M. A. Bobrik, L. Que, Jr., and R. H. Holm, *J. Amer. Chem. Soc.*, **96**, 285 (1974); (b) L. Que, Jr., M. A. Bobrik, J. A. Ibers, and R. H. Holm, *ibid.*, **96**, 4168 (1974).
(10) R. H. Holm, B. A. Averill, T. Herskovitz, R. B. Frankel, H. B. Gray, O. Siiman, and F. J. Grunthaner, *J. Amer. Chem. Soc.*, **96**, 2644 (1974).
(11) E. T. Adman, L. C. Sieker, and L. H. Jensen, *J. Biol. Chem.*, **248**, 3987 (1973).
(12) C. W. Carter, Jr., J. Kraut, S. T. Freer, R. A. Alden, L. C. Sieker, E. Adman, and L. H. Jensen, *Proc. Nat. Acad. Sci. U. S.*, **69**, 3526 (1972).
(13) R. B. Frankel, T. Herskovitz, B. A. Averill, R. H. Holm, P. J. Krusic, and W. D. Phillips, *Biochem. Biophys. Res. Commun.*, in press.
(14) M. Frankel, D. Gertner, H. Jacobson, and A. Zilkha, *J. Chem. Soc.*, 1390 (3960).
(15) W. D. Cash, *J. Org. Chem.*, **27**, 3329 (1962).
(16) V. du Vigneaud, J. L. Wood, and O. J. Irish, *J. Biol. Chem.*, **129**, 171, (1939).
(17) S. W. Chien, Ph.D. Thesis, M.I.T., 1967.

overnight. The white solid remaining was extracted with a total of 2800 ml of boiling ethyl acetate; upon concentrating and cooling the extract, 11.2 g (86%) of Ac-L-Cys-NHMe was obtained: mp 200.5–202.5°; ir (mull) 2550 cm^{-1} (w), ν_{SH}; $[\alpha]^{20}D$ −20.8 (*c* 2.5, DMF). The pmr spectrum was consistent with the indicated formulation. *Anal.* Calcd for $C_6H_{12}N_2O_2S$: C, 40.89; H, 6.86; N, 15.90; S, 18.19. Found: C, 40.92; H, 6.90; N, 15.82; S, 18.27.

Reaction of *p*-Trimethylammoniumbenzenethiol with Ferric Chloride and Sodium Sulfide. Bis(4-dimethylaminophenyl)disulfide[18,19] was converted to bis(4-trimethylammoniumphenyl)disulfide diiodide by treatment with methyl iodide in acetone;[19] mp 152–154° (lit.[19] 151–152°). The disulfide diiodide (11.8 g, 20.0 mmol) was dissolved in 50 ml of water and 200 ml of 3 *N* HCl and stirred with 6.54 g (100 mmol) of zinc dust for 6 hr. After removal of unreacted zinc by filtration, the product was precipitated with 10 ml of 65% HPF_6, washed thoroughly with water, and dried *in vacuo*. This procedure gave 11.4 g (91%) of *p*-trimethylammoniumbenzenethiol hexafluorophosphate as a white powder: mp 174–177°; pmr (DMSO-d_6) −3.59 (Me), −7.73, −7.81, −7.92, −8.00 ppm (ring-H, AB pattern).

A filtered solution of 0.97 g (6.0 mmol) of ferric chloride and 2.03 g (18.0 mmol) of sodium hexafluorophosphate in 50 ml of ethanol was added to a solution of 5.64 g (18.0 mmol) of *p*-trimethylammoniumbenzenethiol and 0.97 g (18 mmol) of NaOMe in 100 ml of methanol. All operations were carried out under a nitrogen atmosphere. Upon mixing a black solid formed immediately. Addition of a solution of sodium hydrosulfide (0.34 g, 6.0 mmol) and sodium methoxide (0.32 g, 6.0 mmol) in 50 ml of methanol resulted in the disappearance of the black solid with formation of a red solid. After stirring for 1 hr the red solid was collected by filtration. After washing with methanol this material was recrystallized from acetonitrile–methanol to give red microcrystals, mp 208–210° dec. *Anal.* Calcd for $[(Me_3NC_6H_4S)_2FeS](PF_6)$, $C_{15}H_{26}F_6N_2PS_3Fe$: C, 38.10; H, 4.62; F, 20.09; N, 4.94; P, 5.46; S, 16.95; Fe, 9.84. Found: C, 38.22; H, 4.44; F, 20.29; N, 5.03; P, 5.25; S, 16.88; Fe, 9.78.

Iron–Sulfur Tetramers. The species $[Fe_4S_4(SC_6H_4NMe_3)_4]^{2+}$ and $[Fe_4S_4(S\text{-}Cys(Ac)NHMe)_4]^{2-}$ were not isolated but were generated in solution by ligand substitution reactions[9] of $[Fe_4S_4(S\text{-}t\text{-}Bu)_4]^{2-}$ using *p*-trimethylammoniumbenzenethiol hexafluorophosphate and *N*-acetyl-L-cysteine-*N*-methylamide, respectively. Several new salts of previously reported tetrameric dianions were prepared by the usual tetramer synthesis.[8] Other compounds were available from previous work.[1,7,8]

$(n\text{-}Pr_4N)_2[Fe_4S_4(SEt)_4]$. *Anal.* Calcd for $C_{32}H_{76}N_2S_8Fe_4$: C, 39.66; H, 7.92; N, 2.89; S, 26.47; Fe, 23.06. Found: C, 39.61; H, 7.88; N, 3.03; S, 26.39; Fe, 22.95.

$(Et_4N)_2[Fe_4S_4(SPh)_4]$. *Anal.* Calcd for $C_{40}H_{60}N_2S_8Fe_4$: C, 45.80; H, 5.78; N, 2.67; S, 24.45; Fe, 21.30. Found: C, 45.96; H, 5.85; N, 2.77; S, 24.27; Fe, 21.16.

$(n\text{-}Pr_4N)_2[Fe_4S_4(SCH_2Ph)_4]$. *Anal.* Calcd for $C_{52}H_{84}N_2S_8Fe_4$: C, 51.31; H, 7.00; N, 2.30; S, 21.07; Fe, 18.35. Found: C, 51.47; H, 6.91; N, 2.41; S, 21.20; Fe, 18.44.

Physical Measurements. Due to the sensitivity of $[Fe_4S_4(SR)_4]^{2-}$ species to oxygen, especially in solution, all manipulations and measurements were carried out under a pure nitrogen atmosphere. Proton resonance spectra were measured at *ca.* 30° on a Varian HA-100 spectrometer. Chemical shifts are relative to a TMS internal standard. As previously,[1] shifts downfield of TMS are taken as negative. Electronic spectra were obtained on a Cary 14 spectrophotometer using quartz cells.

Electrochemical measurements were carried out with a Princeton Applied Research Model 170 electrochemistry system. Solutions were maintained at 25.0 ± 0.1° and unless otherwise indicated contained 0.05 *M* tetra-*n*-propylammonium perchlorate (TPAP) supporting electrolyte and *ca.* 10^{-3} *M* tetramer salt. The cell was of standard three-electrode design containing a dropping mercury (dme) or rotating platinum (rpe) working electrode and an aqueous saturated calomel reference electrode (sce). The sce contacted the base electrolyte nonaqueous solution *via* a compacted filter paper plug and this solution was separated from the sample solution by a medium porosity frit. In the cyclic voltammetry measurements a stationary platinum electrode described elsewhere[20] was used. Eastman Spectrograde acetonitrile was used without further purification. Reagent grade DMSO (Matheson Coleman and Bell) was stored over Linde Type 3A molecular sieves for several days before use. Reagent grade DMF (Baker) was similarly treated and then vacuum distilled from sodium anthracenide. DMSO–water solutions were 4:1 v/v and the pH of the aqueous component was adjusted before mixing to pH 7 or 9 with Tris–Cl buffer. The majority of compounds were examined in DMF using both a dme and rpe. Half-wave potentials were in good agreement, but the characteristics of the current–voltage curves were in general somewhat more satisfactory at the dme and nearly all of the data reported were obtained with this electrode. The precision of $E_{1/2}$ values is ±(5–10) mV.

The insolubility in water of all currently well-characterized salts of the tetramer dianions necessitated measurement of redox properties in nonaqueous or partially aqueous media. In an attempt to provide a basis for comparison of the $[Fe_4S_4(SR)_4]^{2-/3-}$ half-wave potentials in different solvents, the pilot ion method[21–23] was employed to approximate the sce, $KCl|(R_4N^+)(ClO_4^-)$, nonaqueous base electrolyte solution liquid junction potentials (ljp) [$E_{1j} = E_{1/2}(\text{nonaq}) - E_{1/2}(\text{aq})$]. Of the various pilot ion redox couples whose potentials without ljp have been proposed to be independent of medium, the ferrocene–ferricinium ($Fc^{0/+}$) and Tl^+/Tl(Hg) couples have been employed. Reductions of $Fc^+PF_6^-$ and $TlClO_4$ were performed in aqueous solution containing 0.05 *M* tetraethylammonium perchlorate (TEAP): $E_{1/2}$ = +0.171 V ($Fc^{+/0}$, rpe); $E_{1/2}$ = −0.440 V (Tl^+/Tl(Hg), dme). Previously reported values for these couples in aqueous solution are +0.145[24] (0.1 *M* TEAP), +0.160[22] (0.1 *M* $LiClO_4$), and −0.46 V.[25] Potentials of the pilot ion couples were determined under the same conditions as used in the tetramer measurements. The following E_{1j} values (V) were obtained from $Fc^{0/+}$ and Tl^+/Tl(Hg) half-wave potentials: MeCN, +0.25, +0.20; DMF, +0.31, +0.06; DMSO, +0.29, −0.04; DMSO–H_2O (unbuffered), −, −0.01; DMSO–H_2O (pH 9), +0.21, −; DMSO–H_2O (pH 7), +0.20, −. (The Tl^+/Tl(Hg) couple could not be used in the buffered DMSO–H_2O mixtures due to the presence of chloride in the buffer salt.) Apparent junction potentials were larger when obtained from $Fc^{0/+}$ potentials. The values of E_{1j} for the MeCN-aqueous junction is comparable to that carefully determined by Kolthoff and Thomas[24] (*ca.* +0.25 V) but larger than other estimates.[22,23,26] Similarly, the E_{1j} values for the DMSO- and DMF-aqueous junctions determined by using the $Fc^{0/+}$ couple are larger than these quoted by Headridge.[23] Inasmuch as junction potentials will depend to some degree on the physical nature of the solution contact as well as the detailed solution compositions, comparison of the preceding E_{1j} values is obviously of uncertain merit. The pilot ion method suffers from well-recognized deficiencies, and the use of both the $Fc^{0/+}$[22] and Tl^+/Tl(Hg)[26] couples has been criticized. Consequently, the apparent junction potentials estimated by the use of these couples are applied to an assessment of the trend of solvent effects on tetramer half-wave potentials and not to an accurate determination of these potentials without ljp.

Results and Discussion

The electronic spectra and redox properties of an extensive series of tetramers $[Fe_4S_4(SR)_4]^{2-}$ with R = alkyl and aryl have been determined. Results are collected in Tables I–III and Figures 2–5. In all but two cases measurements were performed on isolated salts of the dianions, which were obtained by the tetramer synthesis described earlier.[8] The species $[Fe_4S_4(SC_6H_4NMe_3)_4]^{2+}$ and $[Fe_4S_4(S\text{-}Cys(Ac)NHMe)_4]^{2-}$ were prepared in solution by the ligand substitution reactions considered next.

Ligand Substitution Reactions. The tetramer with

(18) V. Merz and W. Weith, *Chem. Ber.*, **19**, 1571 (1886).

(19) N. V. Khromov-Borisov, V. E. Gmiro, and L. G. Magasanik, *Khim.-Farm. Zh.*, **3**, 21 (1969); *Chem. Abstr.*, **71**, 90989 (1969).

(20) C. E. Forbes, A. Gold, and R. H. Holm, *Inorg. Chem.*, **10**, 2479 (1971).

(21) H.-M. Koepp, H. Wendt, and H. Strehlow, *Z. Electrochem.*, **64**, 483 (1960).

(22) I. V. Nelson and R. T. Iwamoto, *Anal. Chem.*, **35**, 867 (1963).

(23) J. B. Headridge, "Electrochemical Techniques for Inorganic Chemists," Academic Press, New York, 1969, pp 71–80.

(24) I. M. Kolthoff and F. G. Thomas, *J. Phys. Chem.*, **69**, 3049 (1965).

(25) L. Meites, "Handbook of Analytical Chemistry," McGraw Hill, New York, N. Y., 1963, Table 5-23.

(26) J. F. Coetzee and J. J. Campion, *J. Amer. Chem. Soc.*, **89**, 2513, 2517 (1967).

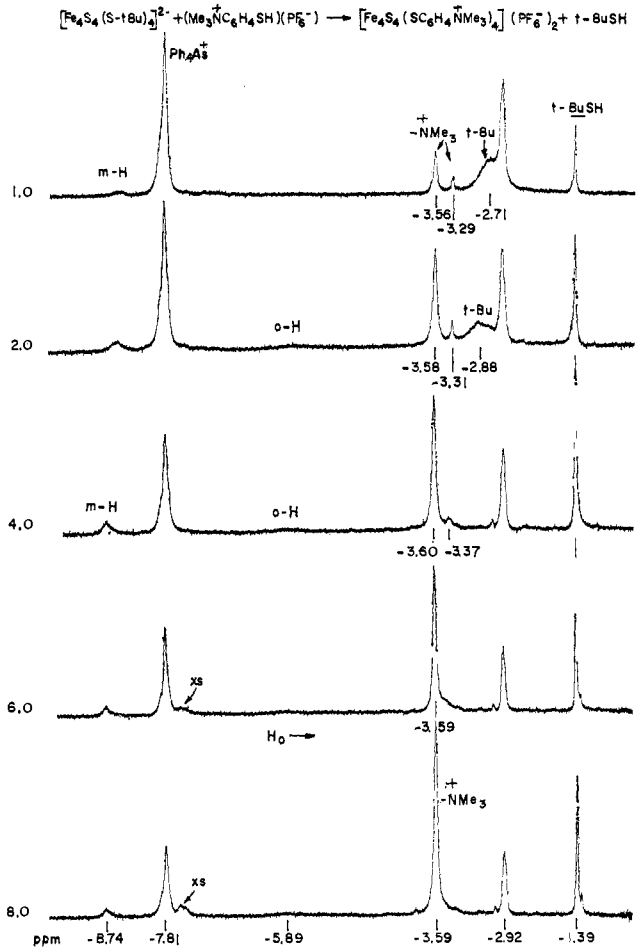

Figure 1. Pmr spectra (100 MHz) for the ligand substitution reaction between $(Ph_4As)_2[Fe_4S_4(S\text{-}t\text{-}Bu)_4]$ and $(p\text{-}Me_3NC_6H_4SH)(PF_6)$ in DMSO-d_6 solution at ~30°. Numerical values at the left are the mole ratios of added thiol to original tetramer. The signal at −2.92 ppm and the weak feature immediately downfield and observable in the lower three spectra arise from protonated solvent and water, respectively. The TMS reference signal has been omitted.

R = SC_6H_4-*p*-NMe_3^+ was required as part of the investigation of the dependence of redox potentials on R substituent constants. Reaction of *p*-trimethylammoniumbenzenethiol hexafluorophosphate with ferric chloride, sodium methoxide, and sodium hydrosulfide as in the usual tetramer synthesis[8] did not afford a salt of $[Fe_4S_4(SC_6H_4NMe_3)_4]^{2+}$. Instead, a material was isolated whose empirical composition, $[FeS(SC_6H_4NMe_3)_2](PF_6)$, and absorption spectrum were not consistent with the expected tetramer. The cationic component of this salt appears to be the dimer $[FeS(SC_6H_4NMe_3)_2]_2^{2+}$, similar to $[FeS(SCH_2)_2C_6H_4]_2^{2-}$,[6] and its physical properties will be reported elsewhere.[27] The required complex was obtained by the ligand substitution reaction (1) taking advantage of the finding[9] that aryl-

$$[Fe_4S_4(S\text{-}t\text{-}Bu)_4]^{2-} + 4Me_3\overset{+}{N}C_6H_4SH \longrightarrow [Fe_4S_4(SC_6H_4NMe_3)_4]^{2+} + 4t\text{-BuSH} \quad (1)$$

thiols readily replace coordinated thiolate in the R = *t*-Bu tetramer. This reaction has been monitored by pmr and electronic[9b] spectroscopy. Pmr spectral changes pursuant to the addition of varying amounts of the thiol salt to a DMSO-d_6 solution of the original tetramer are shown in Figure 1. Increases in the (thiol)/(tetramer) mole ratio result in diminution of the intensity of the coordinated *t*-Bu signal at −2.71 ppm, increase in intensity of the free *t*-BuSH signal at −1.39 ppm, and the emergence of resonances at −5.89 and −8.74 ppm due to coordinated aromatic thiolate. At a ratio of ~6/1 the coordinated *t*-Bu peak has disappeared. This observation, together with the integrated intensities of the free *t*-BuSH *vs.* Ph_4As^+ signals, indicates that full substitution has taken place. Ring proton resonances of excess thiol are evident at ratios of 6/1 or higher.

The pattern of spectral changes observed in Figure 1 is consistent with those found for the addition of other aromatic thiols to solutions of $[Fe_4S_4(S\text{-}t\text{-}Bu)_4]^{2-}$ [9] and indicates that $[Fe_4S_4(SC_6H_4NMe_3)_4]^{2+}$ is fully formed at (thiol)/(tetramer) ratios of ~6/1 or more. The shifting and broadening of the ortho and meta proton signals of coordinated thiolate are similar to those found in the spectra of other phenyl-substituted tetramers, whose isotropic shifts appear to be dominantly contact in origin.[1] For example, the isotropic shifts of the dication (*o*-H, +1.88; *m*-H, −0.78 ppm relative to free thiol) compare closely to those of $[Fe_4S_4(SPh)_4]^{2-}$ (*o*-H, + 1.56; *m*-H, −0.89 ppm) in DMSO-d_6 at 22°.[1] Apparently contact interactions are largely attenuated at the $-NMe_3^+$ group, and methyl resonances of free thiol (−3.59 ppm) and coordinated thiolate are not well resolved at 100 MHz. In DMSO-d_6 solution the product from direct synthesis exhibited methyl and ring proton signals at −3.66 and −9.61 ppm, respectively, which are dissimilar to those of the ligand exchange product. The only peak of uncertain origin in Figure 1 is the resonance immediately upfield of the principal $-NMe_3^+$ feature. As the (thiol)/(tetramer) ratio increases this peak shifts downfield and finally merges with the resonance at −3.59 ppm. It presumably arises from the methyl groups of the thiol cation. Other than to note that the displacement of this signal from its usual diamagnetic position may be due to weak ion pairing with anionic tetramers, its chemical shift cannot be satisfactorily interpreted.

Similar experiments have been performed with the system $[Fe_4S_4(S\text{-}t\text{-}Bu)_4]^{2-}$ –Ac-L-Cys-NHMe. The substitution affinity of acetyl-L-cysteine-*N*-methylamide is comparable with those of aromatic thiols,[9b] and the fully substituted tetramer dianion **2** is formed at a

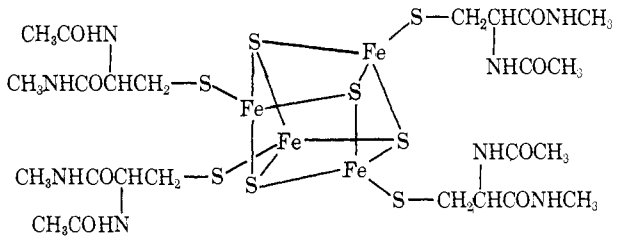

2

(thiol)/(tetramer) ratio of 5 to 7 in DMSO and similar solvents. $[Fe_4S_4(S\text{-}Cys(Ac)NHMe)_4]^{2-}$ has proved difficult to obtain by direct synthesis and is of importance because of the similarity of its thiolate ligands to the protein cysteinyl residues which are coordinated to iron in structure **1**.[11,12] Spectral and voltammetric data for $[Fe_4S_4(SC_6H_4NMe_3)_4]^{2+}$ and $[Fe_4S_4(S\text{-}Cys$-

(27) J. J. Mayerle, S. E. Denmark, J. A. Ibers, and R. H. Holm, results to be submitted for publication.

$(Ac)NHMe)_4]^{2-}$ have been obtained from measurements of solutions containing sufficient thiol (*ca.* eight- to tenfold excess) to ensure complete formation of these tetramers. Pmr properties of the latter complex will be reported subsequently.[28]

Electronic Spectra. As part of the physical characterization of the complexes **1**, their solution spectra have been determined in the 250–700 nm region, which corresponds to that commonly measured for Fd_{ox} and HP_{red} proteins. Attention is first directed toward the results for a series of tetramers in one solvent, DMF. Representative spectra are shown in Figure 2 and data for the principal absorption features are collected in Table I. All species have at least one absorption band

Table I. Principal Electronic Spectral Features of $[Fe_4S_4(SR)_4]^{2-}$ in DMF Solution

R	λ_{max},[a] nm (ϵ_M)
CH_3	297 (22,600), 418 (16,100)
CH_2CH_3[c]	298 (23,300), 420 (17,200)
$CH_2CH_2CH_3$[d]	300 (22,400), 419 (16,600)
$CH(CH_3)_2$[b]	303 (22,100), 421 (17,000)
$CH_2C_6H_{11}$[c]	308 (23,700), 418 (17,800)
$C(CH_3)_3$[b]	303 (21,800), 417 (16,700)
$CH_2C_6H_5$[c]	~286 (sh, 28,800), 420 (18,500)
m-$C_6H_4(CH_2)_2$[b]	370 (12,800), 421 (12,900)
C_6H_5[e]	260 (45,000), 457 (17,700)
p-$C_6H_4N(CH_3)_2$	275 (72,300), 510 (14,300)
p-$C_6H_4N(CH_3)_3^+$[f]	455 (18,800)

[a] 25°. [b] *n*-Bu_4N^+ salt. [c] *n*-Pr_4N^+ salt. [d] Ph_4As^+ salt. [e] Et_4N^+ salt. [f] Prepared by ligand substitution reaction (see text), PF_6^- salt, position of higher energy bands obscured by excess thiol.

in the 400–700 nm region, with the main bands of the aryl-substituted tetramers considerably more red-shifted than those of the tetramers with R = alkyl. The latter are of more interest because of the greater degree of similarity of their thiolate ligands to those in the proteins.

Alkyl-substituted tetramers possess two principal absorption bands in the intervals 417–421 nm and 297–308 nm. A typical spectrum is provided by $[Fe_4S_4(SEt)_4]^{2-}$. Although somewhat red-shifted, the lower energy feature undoubtedly corresponds to the first prominent absorption band[29] in the spectra of 4-Fe[30–32] and 8-Fe[33–35] Fd_{ox} (λ_{max} 390–400 nm) and HP_{red}[36,37] proteins (λ_{max} 388 nm). This point is emphasized by comparison of extinction coefficients of the synthetic tetramers (Table I) with those of the proteins. The most accurate result for the latter appears to be ϵ_{390} 30,600 for *Clostridium acidi-urici* Fd_{ox},[33] corresponding to 15,300 per active site. Other values for Fd_{ox} proteins fall in the range 15,400–16,800 per active site,[31,32,34] and for two HP_{red} proteins ϵ_{388} is 15,300 and 16,100.[36,37] Both Fd_{ox} and HP_{red} proteins possess absorption maxima near 280 nm which are more intense than the lower energy bands. This feature is also present in apoferredoxins[33] and its variable intensity in the two types of proteins as well as between similar ferredoxins[32] has been ascribed to differing aromatic amino acid content. If the 297–308 nm bands of those tetramers which lack aromatic chromophores are also red-shifted compared to the proteins, then the ~280 nm absorptions of Fd_{ox} and HP_{red} derive substantial intensity from the iron–sulfur chromophore.

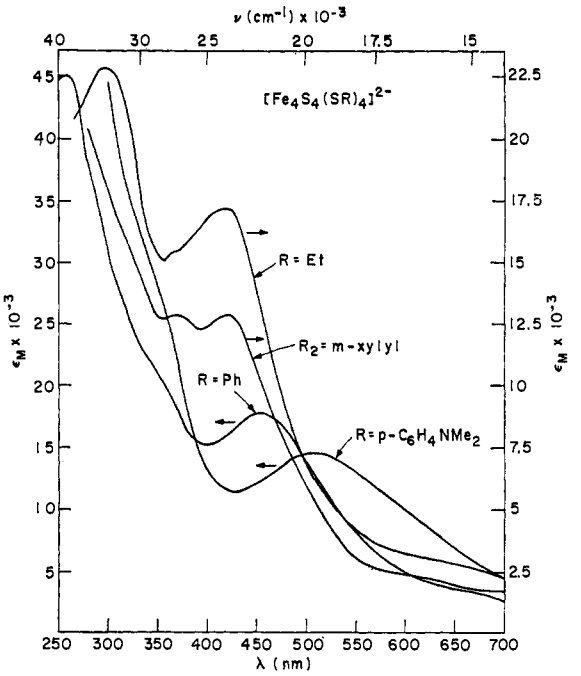

Figure 2. Electronic spectra of $(Me_4N)_2[Fe_4S_4(SC_6H_4\text{-}p\text{-}NMe_2)_4]$, $(Et_4N)_2[Fe_4S_4(SPh)_4]$, $(n\text{-}Pr_4N)_2[Fe_4S_4(SEt)_4]$, and $(n\text{-}Bu_4N)_2[Fe_4S_4(m\text{-}xyl\text{-}S_2)_2]$ in DMF solution at ~25°. The left and right intensity scales refer to the first two and last two compounds, respectively.

In addition to their two intense bands, alkyl-substituted tetramers in solution show a series of weaker absorptions. A weak shoulder is found in the 600–700 nm region and evidence for one or more features at *ca.* 430–500 and 320–400 nm is apparent in most cases. Bands in the first two regions are much better resolved in solid samples at 5°K.[10] An absorption band near 690 nm has been reported in the spectrum of *C. acidi-urici* Fd_{ox} at 77°K[38] and a number of Fd_{ox} proteins[30–35] display shoulders or discrete maxima at wavelengths intermediate between those of their two principal absorptions. CD spectra of HP_{red}[37] and recent MCD spectra of Fd_{ox} proteins,[39] as well as earlier ORD[40a] and CD[40b] results for the latter, reveal that the region 300–600 nm, although dominated by one intense band,

(28) L. Que, Jr., J. R. Anglin, M. A. Bobrik, A. Davison, and R. H. Holm, results submitted for publication.

(29) Unless otherwise noted protein absorption and redox potential data refer to aqueous solution and pH ~7. Citations of these data are selective rather than comprehensive.

(30) J. LeGall and N. Dragoni, *Biochem. Biophys. Res. Commun.*, **23**, 145 (1966).

(31) J. A. Zubieta, R. Mason, and J. R. Postgate, *Biochem. J.*, **133**, 851 (1973).

(32) N. A. Stombaugh, R. H. Burris, and W. H. Orme-Johnson, *J. Biol. Chem.*, **248**, 7951 (1973).

(33) J.-S. Hong and J. C. Rabinowitz, *J. Biol. Chem.*, **245**, 4982 (1970).

(34) K. Gersonde, E. Trittelvitz, H.-E. Schlaak, and H.-H. Stabel, *Eur. J. Biochem.*, **22**, 57 (1971).

(35) S. G. Mayhew, D. Petering, G. Palmer, and G. P. Foust, *J. Biol. Chem.*, **244**, 2830 (1969).

(36) K. Dus, H. DeKlerk, K. Sletten, and R. G. Bartsch, *Biochim. Biophys. Acta*, 140, 291 (1967).

(37) T. Flatmark and K. Dus, *Biochim. Biophys. Acta*, **180**, 377 (1969).

(38) D. F. Wilson, *Arch. Biochem. Biophys.*, **122**, 254 (1967).

(39) D. D. Ulmer, B. Holmquist, and B. L. Vallee, *Biochem. Biophys. Res. Commun.*, **51**, 1054 (1973).

(40) (a) R. D. Gillard, E. D. McKenzie, R. Mason, S. G. Mayhew, J. L. Peel, and J. E. Stangroom, *Nature (London)*, **208**, 769 (1965); (b) N. M. Atherton, K. Garbett, R. D. Gillard, R. Mason, S. G. Mayhew, J. L. Peel, and J. E. Stangroom, *Nature (London)*, **212**, 590 (1966); T. Devanathan, J. M. Akagi, R. T. Hersh, and R. H. Himes, *J. Biol. Chem.*, **244**, 2846 (1969).

Table II. Cathodic Polarography of $[Fe_4S_4(SR)_4]^{2-}$ in DMF Solution[a]

R	$E_{1/2}$, V	2−/3− i_d/C, μA/m*M*	Slope, mV	$E_{1/2}$, V	3−/4− i_d/C, μA/m*M*	Slope, mV
CH_3[b]	−1.294	1.37	−60	−2.024	1.66	−76
CH_2CH_3[c]	−1.331	1.58	−63	−2.038	1.86	−65
$CH_2CH_2CH_3$[d,e]	−1.341	1.57				
$CH(CH_3)_2$[b]	−1.385	1.54	−60	−2.105	1.72	−72
$CH_2C_6H_{11}$[c]	−1.404	1.52	−71	−2.128	2.14	−85
$C(CH_3)_3$[c]	−1.424	1.50	−58	−2.161	1.63	−55
$CH_2C_6H_5$[c]	−1.252	1.43	−64	−1.958	1.82	−94
m-$C_6H_4(CH_2)_2$	−1.391	1.53	−72	−2.027	2.36	∼−85
C_6H_5[f]	−1.039	1.52	−56	−1.748	1.76	−48
p-$C_6H_4CH_3$[g]	−1.086	1.49	−60	−1.761	1.46	−45
p-$C_6H_4N(CH_3)_2$[g]	−1.140	1.73	−71	−1.795	1.23	−42
p-$C_6H_4\overset{+}{N}(CH_3)_3$[h,i]	−0.793	*i*	−52			
p-$C_6H_4NO_2$[g]	−0.695	1.05	−59	−1.25[k]	1.91	
C_6F_5[b,j]	−0.787	2.36	−63			
C_6Cl_5[f,j]	−0.776	2.20	−64			

[a] Measured with dme at 25.0°; potentials *vs.* sce. [b] *n*-Bu_4N^+ salt. [c] *n*-Pr_4N^+ salt. [d] Ph_4As^+ salt. [e] First wave slightly overlapped and second wave obscured by cation reduction. [f] Et_4N^+ salt. [g] Me_4N^+ salt. [h] Dipositive cation, prepared by ligand exchange (see text); PF_6^- salt. [i] Measured with rpe, current consistent with one-electron transfer; second reduction obscured. [j] Acetonitrile solution, additional reductions are not well defined. Diffusion currents are comparable with the value of 2.40 μA/m*M* (slope −62 mV) found for $[Fe_4S_4(SPh)_4]^{2-/3-}$ in acetonitrile. [k] May correspond to ligand reduction.

actually contains three or more transitions. It is concluded that the spectra of $[Fe_4S_4(SR)_4]^{2-}$ in DMF bear a credible relation to those of Fd_{ox} and HP_{red} proteins in aqueous solution and provide further evidence that the iron–sulfur clusters in these systems possess a common total oxidation level.

The first intense transition in all tetramers and those at 297–308 nm in alkyl-substituted tetramers must arise from charge-transfer processes involving excitation of sulfur-based electrons to appropriate acceptor orbitals of the Fe_4S_4 core. Sulfur → metal charge transfer absorptions have recently been assigned in compounds containing tetrahedral Fe(II,III)–S_4 units and have been found to occur in the *ca.* 370–900 nm region.[41] In view of the delocalized electronic structure of $[Fe_4S_4(SR)_4]^{2-}$ [10] and the uncertainty in the nature of the core energy levels, no specific assignments of these transitions can be offered at present.

Lastly, the spectrum of a complex derived from *m*-xylyl-α,α′-dithiol and obtained by the direct tetramer synthesis[1] is noted. This spectrum (Figure 2, R = *m*-xylyl) contains a band (421 nm) characteristic of alkyl-substituted tetramers, albeit of reduced intensity, and a second maximum at 370 nm, which may correspond to the poorly resolved features in the 320–400 nm region of other tetramers. As for tetramers containing phenyl rings, a distinct maximum is not found at ∼300 nm. This spectrum, together with analytical and pmr results given earlier,[1] is considered consistent with the tetrameric formulation $[Fe_4S_4(m\text{-xyl-}S_2)_2]^{2-}$ of proposed structure **3**, having two phenyl rings held roughly parallel to the cluster faces. In this sense the tetramer bears an approximate resemblance to the active sites of *P. aerogenes* Fd_{ox},[11] each of which has one tyrosyl ring similarly positioned and within van der Waals contact. Attempts to obtain crystals of this compound suitable for an X-ray structural study have thus far been unsuccessful.

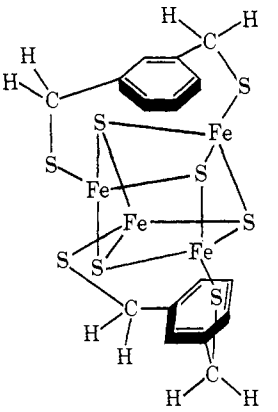

3

Redox Properties. The electron transfer behavior of a series of tetramers $[Fe_4S_4(SR)_4]^{2-}$ has been investigated by polarography in DMF solution. Data are collected in Table II and selected current–voltage curves are shown in Figure 3. The majority of tetramers exhibited two reduction processes in this solvent. Plots of $\log [i/(i_d - i)]$ *vs.* *E* for the first reduction yielded slopes which in nearly all cases are acceptably close to the theoretical value of 59 mV for a reversible one-electron transfer at 25°. The characteristics of the 2−/3− reduction of all tetramers examined in both DMF and acetonitrile are closely similar, with $E_{1/2}$ values (dme) being 40–60 mV more positive in the latter solvent. The first reduction of $[Fe_4S_4(SPh)_4]^{2-}$ was examined in some detail by cyclic voltammetry. The diagnostic current criteria for reversible charge transfer[42] were satisfied, with $i_{p,c}/i_{p,a}$ and the current function $i_p/v^{1/2}$ essentially independent of scan rate in the interval $10 \leq v \leq 200$ mV/sec.[43] However, the theoretical peak potential separation $E_{p,c} - E_{p,a} = 59$ mV is closely approached only at the slower scan rates and increases as *v* increases.[43] This behavior indicates that the reaction is quasi-reversible[42] and subject to both diffusion and charge transfer kinetic effects.

(41) J. V. Pivnichny and H. H. Brintzinger, *Inorg. Chem.*, **12**, 2839 (1973).

(42) R. S. Nicholson and I. Shain, *Anal. Chem.*, **36**, 706 (1964).

(43) At the sweep rates *v* (mV/sec) the following values of $E_{p,c} - E_{p,a}$ (mV), $i_{p,c}/i_{p,a}$ and $i_p/v^{1/2}$ (μA sec$^{1/2}$ mV$^{-1/2}$) were obtained: 10, 61, 1.02, 0.64; 20, 64, 0.99, 0.63; 50, 68, 1.00, 0.65; 100, 72, 1.02, 0.61; 200, 75, 1.00, 0.62. At $v > 500$ mV/sec peak potential separations continue to increase, consistent with quasi-reversible charge transfer.[42]

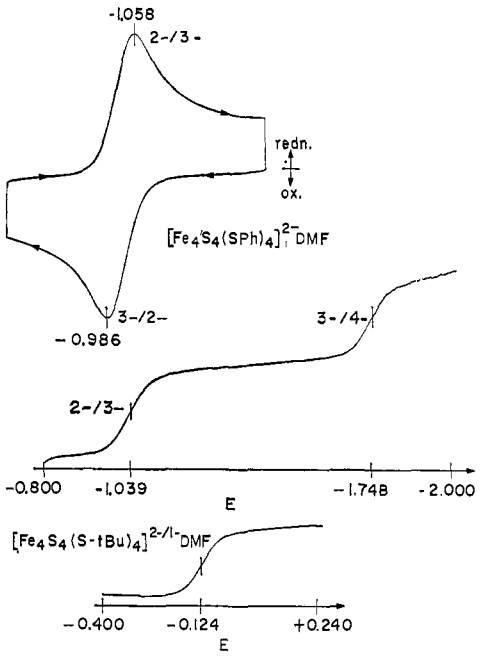

Figure 3. Current–voltage curves for the redox processes of $[Fe_4S_4(SR)_4]^z$ in DMF: upper, cyclic voltammogram for 2−/3− reduction of R = Ph at a stationary Pt electrode (sweep rate 100 mV/sec), conventional polarogram for 2−/3− and 3−/4− reductions of R = Ph at a rpe; lower, 2−/1− oxidation of R = *t*-Bu at a rpe.

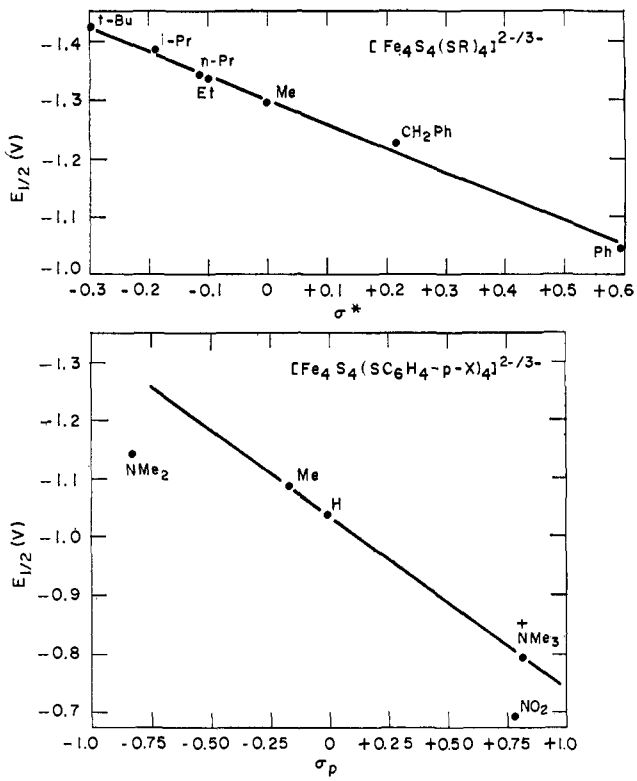

Figure 4. Upper: correlation of half-wave potentials for the 2−/3− process with substituent σ^* values for the series R = alkyl, pH. Lower: correlation of half-wave potentials for the 2−/3− process with substituent σ_p values for the series R = p-C_6H_4X, X = H, Me, NMe_2, NMe_3, NO_2. Potentials were measured in DMF solution (*cf.* Table II).

Coulometric and spectroelectrochemical experiments with the R = CH_2Ph and Ph tetramer dianions have confirmed the one-electron nature and effective reversibility of the first reduction.[44] Half-wave potentials for the 2−/3− process are therefore taken as approximately equal to the normal electrode potentials for the reacting systems, $E_{1/2} \cong E_0$, in the comparison with protein redox potentials given below.

Current–voltage characteristics of the second reduction process are somewhat less satisfactory, with greater variance in diffusion currents and slopes evident. In several cases (*e.g.*, R = Et, *t*-Bu) the data indicate well-behaved reductions at the dme.[45] In addition to the two cathodic waves, the majority of alkyl-substituted tetramers exhibited an anodic process in DMF and acetonitrile at *ca.* −0.3 to +0.1 V. No discrete wave was observed for the phenyl or *p*-tolyl tetramers. The most satisfactory waves were found for $[Fe_4S_4(m\text{-xyl-}S_2)_2]^{2-}$ and $[Fe_4S_4(S\text{-}t\text{-Bu})_4]^{2-}$. That for the latter complex obtained at an rpe (Figure 3) is described by a slope of 56 mV and a diffusion current of 1.44 μA/mM, which is in good correspondence with the value of 1.47 μA/mM for the 2−/3− reduction under the same conditions. Thus the characteristics of the second reduction and the oxidation of a number of tetramers under conventional slow-scan voltammetric conditions closely approach those for reversible one-electron processes. However, the cyclic voltammetry of these processes (Pt electrode) is not consistent with reversible charge transfer, at least in DMF and acetonitrile solutions. Wave shapes reveal the initial oxidation or reduction peak, but the complementary peak is distorted or absent in the reverse scan, suggesting a process of fast electron transfer followed by relatively rapid decomposition.[42]

A significant feature of the 2−/3− process is the dependence of half-wave potentials on the substituent R. The spread of potentials is 0.73 V in DMF (Table II). Potentials become more positive (increasing ease of reduction) as the electron-releasing tendency of the substituents decreases. The trends can be described empirically in terms of the linear free energy correlations with Taft σ^* (R = alkyl, Ph) and Hammett σ_p (R = Ph, p-C_6H_4X) constants[47] plotted in Figure 4. Least-squares fits of the data yield the following relationships: $E_{1/2}$ (V) = $0.411\sigma^* - 1.30$, and $E_{1/2}$ (V) = $0.295\sigma_p - 1.04$. The latter equation does not include the points for the groups X = NMe_2 or NO_2, whose resonance properties frequently cause deviation from linear free energy relationships. Similar correlations for reversible half-wave potentials of other types of metal complexes are described elsewhere.[48]

Electron-Transfer Series and Protein Oxidation Levels. The polarographic evidence indicates the existence of the four-membered electron transfer series $[Fe_4S_4$-

(44) These results will be presented in a forthcoming report[13] dealing with the properties of $[Fe_4S_4(SR)_4]^{3-}$.

(45) Noting the report[46a] that the highly reduced tetramer $[Fe_4S_4(tfd)_4]^{4-}$ reacts directly with nitrogen, the polarography of $[Fe_4S_4(SEt)_4]^{2-}$ was also examined in DMF under an argon atmosphere. The current–voltage characteristics were insignificantly different from those in Table II obtained under a nitrogen atmosphere. *In situ* generation of $[Fe_4S_4(SR)_4]^{4-}$ by a synthetic reaction has recently been described.[46b]

(46) (a) E. E. van Tamelen, J. A. Gladysz, and J. S. Miller, *J. Amer. Chem. Soc.*, **95**, 1347 (1973); (b) G. N. Schrauzer, G. W. Kiefer, K. Tano, and P. A. Doemeny, *ibid.*, **96**, 641 (1974).

(47) J. Hine, "Physical Organic Chemistry," 2nd ed, McGraw-Hill, New York, N. Y., 1962, Chapter 4.

(48) G. S. Patterson and R. H. Holm, *Inorg. Chem.*, **11**, 2285 (1972), and references therein.

Table III. Solvent Dependence of Spectral and Redox Properties of $[Fe_4S_4(SR)_4]^{2-}$

R	Solvent	λ_{max},[a] nm (ϵ_M)	$E_{1/2}$,[b] V 2−/3−	Slope	$E_{1/2}$ (corr),[b,c] V 2−/3−
Ac-Cys-NHMe[d]	DMF	298 (21,300), 413 (16,200)	−1.067[g]	−71	−1.39[k]
	DMSO	295 (21,900), 414 (16,800)	−1.007[h]	−75	−1.30[l]
	DMSO–H_2O,[e] pH 9	294 (20,700), 410 (15,600)	−0.932	−81	−1.14
	DMSO–H_2O,[e] pH 7	293 (21,500), 410 (15,700)	−0.895	−59	−1.10
	DMSO–H_2O[f]		−0.912	−62	*m*
C_6H_5	DMSO	259 (41,400), 458 (17,600)	−0.936[i]	−65	−1.23[n]
	DMSO–H_2O,[e] pH 9	258 (44,300), 457 (17,700)	−0.881	−53	−1.09
m-$C_6H_4(CH_2)_2$	DMSO	369 (13,900), 423 (13,900)	−1.314[j]	−63	−1.60[o]
	DMSO–H_2O,[e] pH 7	370 (13,500), 416 (13,300)			

[a] Principal bands. [b] *Vs.* sce at 25.0°. [c] Corrected for liquid junction potential using $Fc^{0/+}$ data. [d] Prepared by ligand substitution. [e] 4:1 v/v. [f] Unbuffered, 0.05 *M* TEAP. Additional reductions (V): [g] −1.66; [h] −1.73; [i] −1.70; [j] −2.07. $E_{1/2}$ (corr) values (V) using $Tl^+/Tl(Hg)$ data: [k] −1.13; [l] −0.97; [m] −0.91; [n] −0.90; [o] −1.28.

$(SR)_4]^z$ (2), with chemical[13] and electrochemical reversibility most satisfactorily established for the $z = 2-/3-$ couple. The proposed relationships of the total oxidation levels of the protein active sites with those of the synthetic tetramers are indicated by columns a, b, and c. The nonbracketed forms of the

$$\begin{array}{ccccc} [Fe_4S_4(SR)_4]^{4-} & \longleftrightarrow & & & \\ [Fe_4S_4(SR)_4]^{3-} & \rightleftharpoons & [Fe_4S_4(SR)_4]^{2-} & \longleftrightarrow & [Fe_4S_4(SR)_4]^{-} \\ Fd_{red} & \rightleftharpoons & Fd_{ox} & & [Fd_{s\text{-}ox}] \\ [HP_{s\text{-}red}] & \rightleftharpoons & HP_{red} & \rightleftharpoons & HP_{ox} \\ (a) & & (b) & & (c) \end{array} \quad (2)$$

proteins are doubtless those involved *in vivo*[5] and have been isolated or produced under *in vitro* conditions.[3-5] The relationships in (b) are supported by the electronic spectral data presented here together with other spectroscopic and magnetic evidence.[1,7,9a] Those in (a) are substantiated by similar results.[13] From (b) and the known one-electron oxidation of HP_{red},[36] the relationships in column c follow. Earlier we had suggested a two-electron difference between Fd_{red} and HP_{ox}[49] and independently Carter, *et al.*,[12] have proposed the "three-state hypothesis" which is entirely equivalent to the relationships above. These relationships suggest the existence of two nonphysiological oxidation levels of the proteins indicated in brackets. Recently, Cammack[50] has demonstrated the existence in aqueous DMSO solution of a "superreduced" form of the *Chromatium* HP protein, $HP_{s\text{-}red}$, whose properties are consistent with the grouping in (a). The "superoxidized" form of a ferredoxin protein has not yet been detected. The most important conclusion to be drawn from the series (2) is that the oxidation levels of the synthetic tetramers encompass all of those currently known for the 4- and 8-Fe proteins.

Solvent Effects on Spectral and Redox Properties. While structural and electronic properties of $[Fe_4S_4(SR)_4]^{2-}$ described here and elsewhere[1,7-10,13] are sufficiently close to those of Fd_{ox} and HP_{red} proteins to render the dianions legitimate active site analogs, there are some important differences. The red shifts of the two principal absorption bands of the synthetic tetramers have already been noted. Half-wave potentials for the $2-/3-$ process of the R = alkyl species in DMF range from −1.25 to −1.42 V. Taking $[Fe_4S_4(SEt)_4]^{2-}$ as an example, its potential *vs.* the aqueous sce when corrected to the standard hydrogen electrode (she) is −1.33 + 0.25 = −1.08 V. In contrast, the potentials E_0' for 4- and 8-Fe ferredoxins fall near −0.40 V,[3,31,32,51-53] with the apparent extremes among characterized proteins being −0.33 (*D. gigas* Fd[31]) and −0.49 V (*Chromatium* Fd[52]). Solvent and ligand structural effects on the redox properties of the synthetic tetramers have been examined, employing primarily $[Fe_4S_4(S\text{-}Cys(Ac)\text{-}NHMe)_4]^{2-}$ (**2**) in DMF, DMSO, and 80% DMSO–H_2O solutions. The latter solvent mixture was selected because the red and s-red forms of *Chromatium* HP protein have been produced in it.[50] Spectral and half-wave potential data are summarized in Table III.

The electronic spectra of **2** in the various solvents reveal the two principal bands found for other alkyl-substituted tetramers. However, these bands are shifted to slightly higher energies, especially in aqueous DMSO. Several spectra are displayed in Figure 5. The maximum at 410 nm is close to that (406 nm) observed for HP_{red} in the same solvent.[50] Small solvent effects on the spectra of the R = Ph and *m*-xylyl tetramers have also been found.

The half-wave potentials for the $2-/3-$ electron transfer process of **2** exhibit an apparent solvent dependence with the values becoming less cathodic in the order DMF > DMSO > DMSO–H_2O. The least negative value is found in 80% DMSO–H_2O (pH 7). To ascertain whether the potential shifts were influenced by liquid junction potential effects, the magnitudes of E_{lj} were investigated using the pilot ion method[21-23] and the reversible couples $Fc^{0/+}$ and Tl^+/Tl (Hg) as described in the Experimental Section. Values of $E_{1/2}$ (corr), half-wave potentials corrected for apparent liquid junction potentials using $Fc^{0/+}$, are entered in the last column of Table III, which also contains footnoted values obtained from the Tl^+/Tl-(Hg) couple. Although the values of E_{lj} obtained from the two pilot ion couples are not in good agreement for all solvents, the half-wave potentials corrected with either couple exhibit the same solvent dependence as the uncorrected values. Thus the trend in $E_{1/2}$ values is presumably a real effect. Corrected half-wave potentials are included in Table III only to illustrate this point and are not intended as accurate $E_{1/2}$ values without liquid junction potential. If, however, they

(49) T. Herskovitz, B. A. Averill, R. H. Holm, and J. A. Ibers, Abstracts of the 15th International Conference on Coordination Chemistry, Toronto, Canada, June 1972, p 1.

(50) R. Cammack, *Biochem. Biophys. Res. Commun.*, **54**, 548 (1973).

(51) K. K. Eisenstein and J. H. Wang, *J. Biol. Chem.*, **244**, 1720 (1969).

(52) B. Bachofen and D. I. Arnon, *Biochim. Biophys. Acta*, **120**, 259 (1966).

(53) K. Tagawa and D. I. Arnon, *Biochim. Biophys. Acta*, **153**, 602 (1968).

are accepted as approximations to these values, they serve as a starting point for a rough comparison with protein E_0' potentials in water. When referenced to the she, the corrected half-wave potentials in 80% DMSO-H_2O (aqueous component pH 7 or 9 or unbuffered) fall in the range of *ca.* −0.7 to −0.9 V. For the $HP_{red}/HP_{s\text{-}red}$ process in the same solvent mixture, it has been estimated that the midpoint potential is $E_m \leq -0.64$ V,[50] near the lower end of the range. However, E_0' values for Fd_{ox}/Fd_{red} determined by potentiometry are less negative (*vide supra*) than this value and *ca.* 0.2–0.6 V more positive than those for **2**. Similarly, the limited polarographic data for 8-Fe proteins in aqueous solution indicate less negative potentials for the proteins compared to the synthetic tetramers. For *C. pasteurianum* Fd_{ox}/Fd_{red} at pH 7 Weitzman, *et al.*,[54] claim $E_{1/2} = -0.57$ V (−0.32 V *vs.* she), and for *Veillonella alcalescens* Fd_{ox}/Fd_{red} at pH 7.6 Dalton and Zubieta[55] report $E_0 = -0.41$ V for a reversible two-electron process.

The principal conclusions drawn from the electrochemical studies are the following: (i) potentials of the $[Fe_4S_4(SR)_4]^{2-/3-}$ couples are reversible or nearly so and can be linearly correlated with electronic substituent constants of R; (ii) $[Fe_4S_4(SR)_4]^{2-}$ with R = alkyl reduce at substantially more negative potentials than do the 4- and 8-Fe ferredoxins; (iii) half-wave potentials for $[Fe_4S_4(S\text{-}Cys(Ac)NHMe)_4]^{2-/3-}$ are somewhat solvent dependent and, of the solvents employed, are least negative in 80% DMSO-H_2O; (iv) the DMSO-H_2O potentials in (iii) are near that estimated for $HP_{red}/HP_{s\text{-}red}$ in the same solvent mixture but are *ca.* 0.2–0.6 V more negative than E_0' values for Fd_{ox}/Fd_{red} in water. Conclusions ii–iv are offered with due provision that comparisons of potentials measured in different solvents by different methods are necessarily imprecise. More accurate comparisons should result from anticipated voltammetric measurements of proteins and analogs in the same solvent. However, these conclusions are considered sufficiently firm to indicate a dependence of tetramer redox potentials on solvent and, more definitely, on the presence or absence of a polypeptide component with its attendant environmental and structural effects on the redox centers when the proteins possess their normal (aqueous) tertiary structure. The influence of the polypeptide can be seen from conclusions (ii) and (iv) and by the ready reduction of Fd_{ox} but not HP_{red} with dithionite in aqueous solution. In addition, the tertiary structure of a particular protein can be perturbed by solvent effects so as to change its redox properties, as shown by pmr studies of *Chromatium* HP[56] in aqueous DMSO. In this medium HP_{red} can be reduced to $HP_{s\text{-}red}$.[50]

As noted above, structural[7,8,9b] and electronic[1,7,10,13] properties of the synthetic tetramer dianions and trianions, together with the electronic spectral data for the former reported herein, establish the relationships (b) and (a) in the electron transfer series (2). It is on the basis of close similarities of properties which support these relationships that we have designated the synthetic tetramers as active site analogs. The relationships in (2) involve *fixed total oxidation levels* of the synthetic species and the proteins whose electronic characteristics, at least for (b), appear to be intrinsic to the $[Fe_4S_4(SR)_4]$ cluster. The preceding comparisons of redox potentials, although not quantitative at this stage, make it clear that protein structure and environment effect a significant contribution to the values of these potentials. The same observation applies to the 2-Fe active site analog $[FeS(SCH_2)_2C_6H_4]_2^{2-}$,[6] whose first reduction potential is substantially more negative than E_0' values for 2-Fe proteins.[3c] Inasmuch as the potentials will depend upon molecular free energy changes associated with electron transfer, *i.e.*, upon factors extrinsic to the Fe–S clusters, discrepancies between values for synthetic tetramers and proteins are not unexpected. While the former possess the array of total oxidation levels found in the 4-Fe and 8-Fe proteins, they cannot as yet be said to reproduce in a semiquantitative sense that functional property of Fd proteins manifested in their aqueous redox potentials. The differences in potentials are considered potentially as instructive as the similarities in properties between fixed oxidation levels in the series (2). Future work will be directed toward elucidating those factors which control values of redox potentials, primarily by examination of proteins in normal and denatured conformations and synthetic tetramers derived from cysteinyl polypeptides.

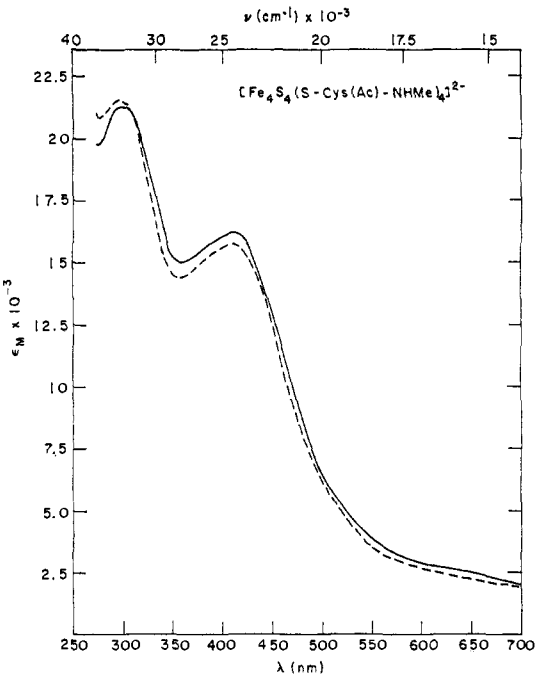

Figure 5. Electronic spectra of $[Fe_4S_4(S\text{-}Cys(Ac)NHMe)_4]^{2-}$ at ~25°: (—) DMF solution, (- - - -) 4:1 v/v DMSO-H_2O (pH 7) solution.

Lastly, the collective electronic characteristics of $[Fe_4S_4(S\text{-}Cys(Ac)NHMe)_4]^{2-}$ described here and elsewhere[9a,28] reveal it to be the closest representation of the Fd_{ox} and HP_{red} active sites among the various synthetic tetramers examined thus far.

Acknowledgment. This research was supported by National Institutes of Health Grant GM-19256. We thank Dr. W. D. Phillips for communication of results prior to publication.

(54) P. D. J. Weitzman, I. R. Kennedy, and R. A. Caldwell, *FEBS (Fed. Eur. Biochem. Soc.) Lett.*, 17, 241 (1971).
(55) H. Dalton and J. Zubieta, *Biochim. Biophys. Acta*, 322, 133 (1973).
(56) W. D. Phillips, C. C. McDonald, M. Poe, and R. Cammack, results to be submitted for publication.